FUZZY IMAGE REGIONS FOR QUANTITATIVE LAND COVER ANALYSIS

Ivan Lizarazo

Cadastral and Geodetics Engineering Department, NIDE Group
University Distrital Francisco Jose de Caldas
Carrera 7 No. 40-53, Bogota, COLOMBIA
ilizarazo@udistrital.edu.co

Commission IV/4

KEY WORDS: impervious surfaces areas, fuzzy segmentation, quantitative land cover

ABSTRACT:

Fuzzy Image Regions were proposed recently as an alternative GEOBIA method for conducting qualitative land cover classification. In this paper, these fuzzy segments are applied for estimation of quantitative (i.e. compositional) land cover. The method comprises three main stages: (i) fuzzy segmentation to create segments with indeterminate boundaries and uncertain thematic allocation; (ii) feature analysis to evaluate contextual properties of fuzzy image regions; and (iii) final regression to estimate compositional land cover. The method is implemented using advanced machine learning techniques and tested in a rapidly urbanizing area using Landsat multispectral imagery. Experimental results suggest that the method produces accurate sub-pixel characterization of land cover classes. Thus, the proposed method is potentially useful for bridging the gap between the traditional quantitative and qualitative perspectives of remote sensing image analysis.

1 INTRODUCTION

Significant research in geographic object-based image analysis (GEOBIA) aims to improve qualitative classification of remotely sensed imagery. Such a trend can be noticed in recent peer-reviewed GEOBIA related journals (Hay and Blaschke, 2010). A large percentage of most recent articles focus on evaluating advantages of GEOBIA classifications over traditional pixel-based classifications, see, for example, (Johansen et al., 2010, Kim et al., 2010, Lizarazo and Barros, 2010). GEOBIA classifications are esentially qualitative classifications of land cover, which allocate discrete labels to pixels. This classification type has demonstrated to be useful in different applications including thematic mapping and change detection in rural and urban environments (Jensen, 2005).

In contrast to qualitative land cover classification, which allocates discrete class labels to pixels, a quantitative land cover classification assigns continuous values expressing class composition percentages (Clapham, 2005). As quantitative classifications estimate sub-pixel land cover classes, they may be, in many cases, much more useful than qualitative classifications. In addition, a quantitative classification seems to be an appealing way to represent the spectral hetereogeneity within land cover classes present in imagery at several spatial resolutions (Fisher and Arnot, 2007). Examples of successful application of quantitative classification of land cover include urbanization monitoring in urban and suburban watersheds (Clapham, 2005, Goetz and Jantz, 2006).

Impervious surfaces is an indicator of the degree of urbanization as well as a major indicator of environmental quality (Arnold and Gibbons, 1996). Impervious surfaces are anthropogenic features through which water cannot infiltrate into the soil, such as roads, driveways, sidewalks, parking lots, and rooftops (Weng, 2007). Digital extraction of impervious surfaces from medium spatial resolution images has been demonstrated difficult due to the mixed pixel problem (Clapham, 2005). Current approaches for impervious surfaces mapping make use of automated masking, visual interpretation and pixel-based regression algorithms (Clapham, 2005, Jantz et al., 2005). Such approaches produce very accurate results but they are labour intensive and time consuming methods (Lizarazo, 2010).

This paper explores the potential of Fuzzy Image Regions Method (FIRME) for quantitative classification of land cover. FIRME was recently proposed as a new GEOBIA method for qualitative classification of urban land cover (Lizarazo and Barros, 2010). Fuzzy image regions are image objects with indeterminate boundaries and uncertain thematic content. These image regions represent a much more general concept than the crisp image objects traditionally used in GEOBIA. In this paper, the FIRME approach is applied for estimation of impervious surface areas (ISA). This works aims to determine whether the inclusion of several spatial and spectral properties of fuzzy image regions contributes to improve the estimation of ISA values.

2 DATA

The study area is a small watershed located in Montgomery County, Maryland, USA. Impervious surface mapping is based on two Landsat Thematic Mapper (TM) images from 1990 and 2000 respectively: Landsat 5-TM of 3 May 1990, and Landsat 5-TM of 8 May 2000. These Landsat images correspond to the world reference system (WRS) path 15, row 33. These images, available from the USGS Earth Resources Observation and Science Center website (http://glovis.usgs.gov), include seven spectral bands as follows:

Band 1: 450 - 520 nm (Blue).
Band 2: 520 - 600 nm (Green).
Band 3: 630 - 690 nm (Red).
Band 4: 760 - 900 nm (Near infrared).
Band 5: 1550 - 1750 nm (Mid-Infrared).
Band 6: 10400 - 12500 nm (Thermal infrared).
Band 7: 2080 - 2350 nm (Mid-infrared).

Of the two Landsat TM images used, the thermal band (band 6) was excluded prior to impervious surface estimation due to its

(a) (b)

Figure 1: True color composition of two dates of Landsat images of the study area: (a) RGB321 of Landsat-TM 1990, and (b) RGB321 of Landsat-TM 2000.

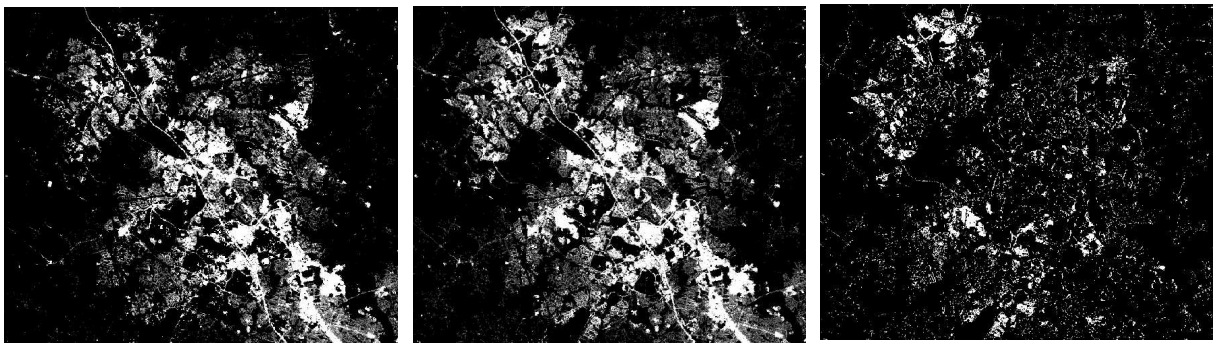

(a) (b) (c)

Figure 2: Impervious surface area (ISA) maps for the study area produced by WHRC: (a) ISA 1990, (b) ISA 2000, (c) Urban development between 1990 and 2000. These maps are used in this experiment as ground reference.

coarse spatial resolution. The six remaining bands are provided in a UTM WGS 84 projection with pixel size of 28.5 meters at 50 meters RMSE absolute positional accuracy. The experimental area covers 655 x 560 pixels (aprox. 297.93 km^2) over the towns of Germantown and Gaithersburg. Figures 1 (a) and (b) show true colour compositions of theses images which are Landsat L1G products, i.e. radiometrically and geometrically corrected images with radiance pixel values scaled to byte values. Due to brightness differences, the increase that occurred in developed land between the two dates is not completely apparent (urbanization correspond roughly to the white and grey coloured areas). The study area was selected because of the availability of very accurate information on impervious surfaces for the time period under consideration (Jantz et al., 2005).

The impervious surface information was available from an extensive study on urbanization in the Chesapeake Bay Watershed, where (Jantz et al., 2005) obtained accurate impervious surface areas (ISA) maps at 30 m spatial resolution for 1990 and 2000. These maps represent impervious surfaces (roofs, streets, sidewalks, etc) as a *continuous* variable, with values ranging from 0% (no impervious) to 100% (completely impervious). The study also produced an accurate analysis of change, using both automated and manual (visual-screening) techniques, and also bare soil areas masking.

These impervious surface area (ISA) maps are publicly available from the Woods Hole Research Center (WHRC). These ISA maps, along the image corresponding to the amount and location of change in the built environment, between 1990 and 2000, are shown in Figure 2. In addition to this, qualitative land cover maps for the same dates are available from the mid-Atlantic Regional Earth Science Applications Center (MA-RESAC) (Jantz et al., 2005). These thematic maps represent five land cover categories: water, urban, grass, trees and bare soil. In this study, both ISA and qualitative thematic maps were used as ground reference for training sample collection and accuracy evaluation. The qualitative land cover maps are used here to get the labeled training samples required to produce one fuzzy image region per land cover class. Then, the ISA maps are used to get the quantitative training samples required to infer quantitative impervious surface area values.

3 METHODS

Figure 3 shows the image analysis workflow for estimating impervious surface area using the FIRME approach. Similarly to the procedure proposed for qualitative classification (Lizarazo and Barros, 2010), it involves three main stages: (i) fuzzy segmentation; (ii) feature analysis; and (iii) defuzzification (i.e. regression). The main difference here is that, in the case of quantitative classification, the final result is a continuous value representing compositional land cover (i.e. imperviousness) rather than a discrete land cover class label. Therefore, the last stage is not a *classification* task but a *regression* task. For a detailed explanation of the different types of fuzzy image regions, a review of the FIRME approach (Lizarazo and Barros, 2010) is suggested.

3.1 FIRME Segmentation

Before starting this stage the two Landsat-TM images were normalized radiometrically to reduce the effect of brightness differences. For such a task, the *histogram matching* technique (Jensen, 2005) was used to *match* the intensities of the six channels of the 2000 scene to the 'standard' 1990 scene.

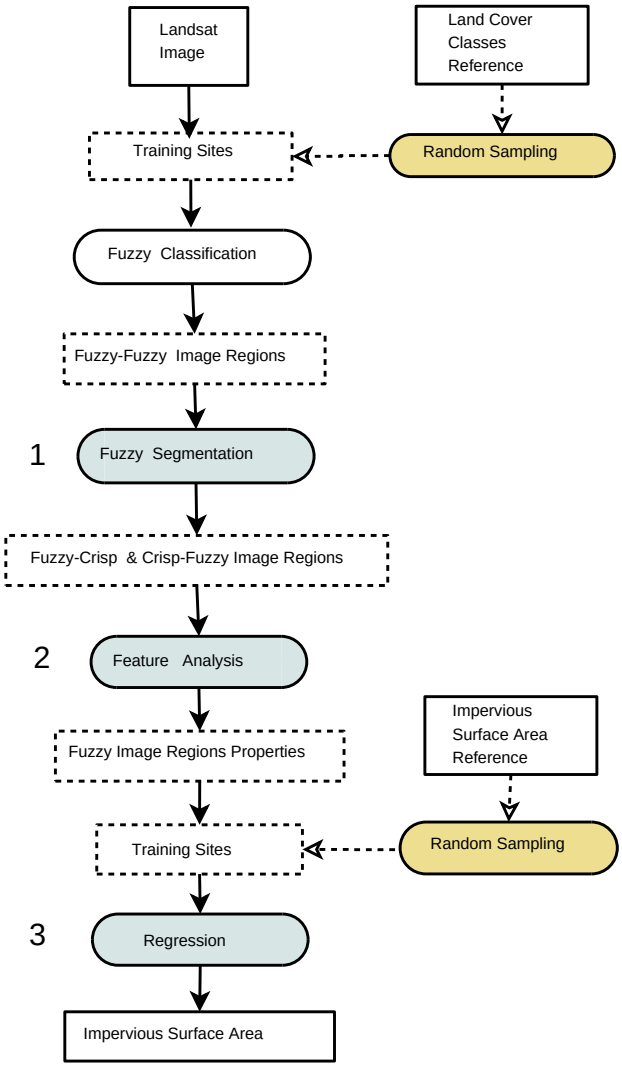

Figure 3: Sequence of stages used for quantitative classification in the FIRME approach: (1) Fuzzy segmentation, (2) Feature Analysis, and (3) Regression.

For the *fuzzy segmentation* stage, a supervised Generalized Additive Model (GAM) regression technique was used. A generalized additive model (GAM) is a special case of a generalized linear model (GLM) in which part of the linear predictor is specified in terms of a sum of smooth functions of predictor variables. The exact parametric form of these functions is unknown as is the degree of smoothness appropriate for each of them (Wood, 2006). While general linear models emphasize the estimation and inference for the model parameters, GAM focuses on exploring data non-parametrically. The strength of GAM is its ability to deal with highly non-linear and non-monotonic relationships between the response variable and a set of explanatory variables (Hastie et al., 2009). In general, a GAM model can be expressed as:

$$Y = S_0 + \sum S_k(X_k) + \epsilon_k \quad (1)$$

where S_0 is the intercept, $S_k(X_k)$ is a non-parametric smoothing function for the k^{th} independent variable $X(k = 1, 2, ..., p)$, and ϵ_k are independent and identically distributed (i.i.d.) $N(0, \sigma^2)$ random variables. The only underlying assumption is that the smoothing functions in GAM are additive.

GAM models have been applied in remote sensing studies related to stochastic simulation of land cover change (Brown et al., 2002) and model-assisted estimation of forest resources (Opsomer et al., 2007).

The supervised GAM regression model was fitted using *land cover memberships* as dependent (response) variable and six *normalized* bands as predictor variables. The GAM technique was applied to create individual regression models from categorical training samples randomly sampled from the available land cover maps. For creating each regression model, the GAM technique was applied using the one-against-all technique (Hastie et al., 2009). A random sample of 1000 pixels was used to obtain training pixels for each land cover. Training samples were assigned either 100 (full membership) or 0 (null membership) to each land cover. Once individual predictions were undertaken for every land cover, a sum-to-one constraint was applied to membership values to interpret fuzzy image regions as compositional classes.

This stage produced five fuzzy-fuzzy image regions: *water*, *urban*, *grass*, *trees* and *soil*, which are shown in Figure 4. Then, these fuzzy-fuzzy image regions were transformed into three new images: (i) crisp image regions, (ii) crisp-fuzzy image regions, and (iii) fuzzy-crisp image regions (using membership values of 0.60 as threshold). These image regions are depicted in Figure 5.

The crisp image C was obtained using a logical union operator referred to as the fuzzy t-conorm MAX operator (Ross, 2004), and defined as follows:

$$C = \mu_{i1} U \mu_{i2} \ldots U \mu_{ic} = max(\mu_{i1}, \mu_{i2}, \ldots, \mu_{i3}) \quad (2)$$

where $max()$ indicates the largest membership value of the i^{th} pixel or neighborhood. Then, contiguous pixels belonging to the same class were clumped and sieved.

The crisp-fuzzy (CF) image was obtained by keeping the boundary of crisp image regions and replacing their interior values (i.e. the largest membership value) with the original membership values at each fuzzy image region. Finally, the fuzzy-crip image (FC) was created by the union of a crisp interior (defined by using the 0.60 membership value as threshold) and the conditional boundary represented by the confusion index (referred to as CI, and explained in the next section) using the following statement: IF $MAX >= 0.60$, THEN $FC = MAX$, OTHERWISE $FC = CI$.

3.2 Feature Analysis

The *feature analysis* stage aims to identify spatial and spectral properties of fuzzy image regions. Contextual relationships between fuzzy image regions can be measured to uncover potential underlying structural information. In addition, geometric and spectral properties of fuzzy image regions can provide clues to resolve spectral confusion between land cover classes.

Contextual relationships were evaluated using the confusion index (CI) (Burrough et al., 1997):

$$CI = 1 - \left[\mu_{maxi} - \mu_{(max-1)i}\right]. \quad (3)$$

where μ_{maxi} and $\mu_{(max-1)i}$ are, respectively, the first and second largest membership value of the i^{th} pixel. The CI measures the overlapping of fuzzy classes at any point and provides insight for further investigating the sites with high membership values to more than one class (Bragato, 2004). CI values are in the range $[0, 1]$, values closer to 1 describe zones where overlapping is critical.

In addition, the information entropy (H) was evaluated at each pixel of the fuzzy image regions as follows (Gonzalez, 2008):

$$H = -\sum_{i=1}^{n} p(x_i) \log p(x_i) \quad (4)$$

where $p(x_i)$ is the probability for each digital number (or intensity level) in the image under consideration (obtained from a histogram of the image intensities), and $\log$ is the natural logarithm with base $e = 2.718282$. Then, the entropy of the full set of fuzzy image regions was summarized using the entropy index (ENTRO) (Gonzalez, 2008):

$$ENTRO = \sum_{c=1}^{m} H_i)/log(128) \quad (5)$$

where m is the number of fuzzy image regions (or land cover classes of interest).

Mean values of spectral bands TM-1, TM-3 and TM-4 within crisp image regions were evaluated as spectral indices. Finally, a geometry attribute, representing the perimeter area ratio was calculated at every crisp image region. The feature analysis stage therefore outputs three contextual indices per date, the confusion index (CI), the entropy index (ENTRO), and the shape index (SHAPE), and two spectral indices, MEAN B1 and MEAN-B2. These indices are shown in Figures 6 and 7.

3.3 Regression

For the final *regression* stage, the estimation of impervious surface area within individual pixels was conducted using thirteen predictors as follows:

1. fuzzy image regions water
2. fuzzy image region urban
3. fuzzy image region grass
4. fuzzy image region trees
5. crisp image regions,
6. crisp-fuzzy image regions,

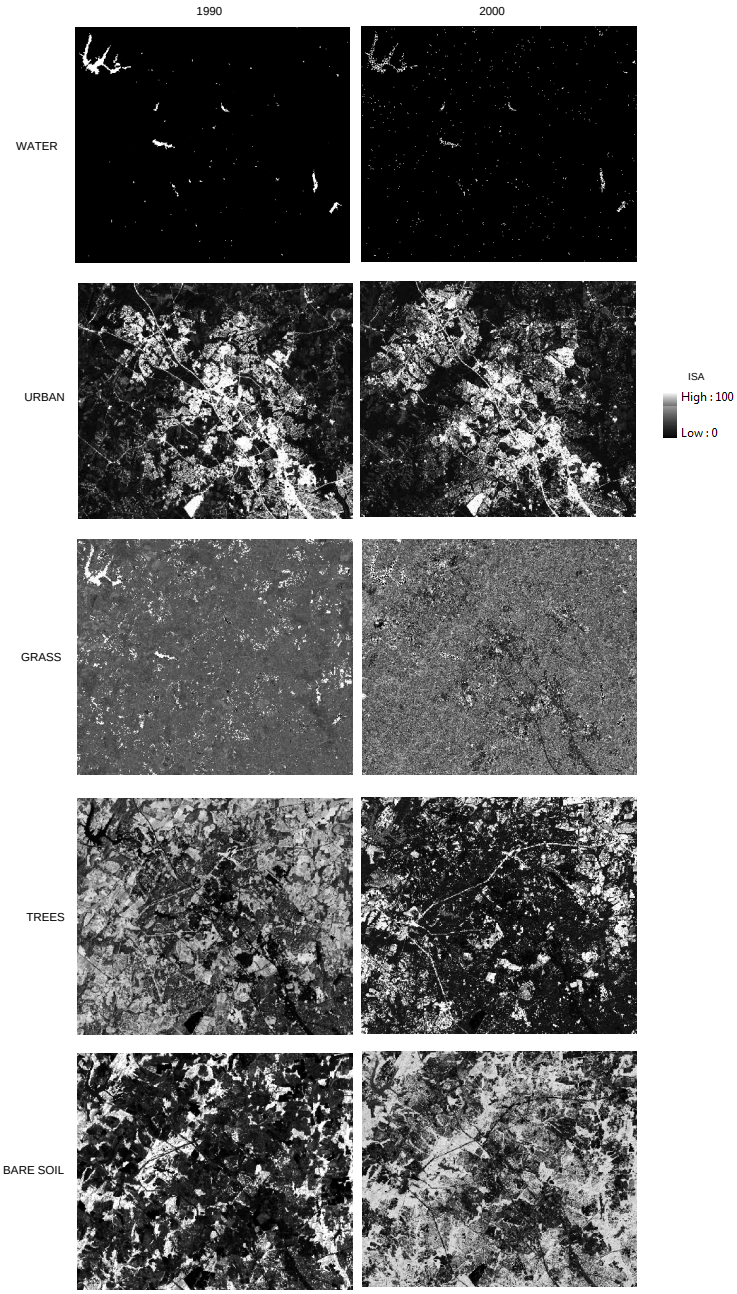

Figure 4: Fuzzy-fuzzy image regions obtained in the fuzzification stage for the 1990 and 2000 dates. From top to botton: water, urban, grass, trees and bare soil.

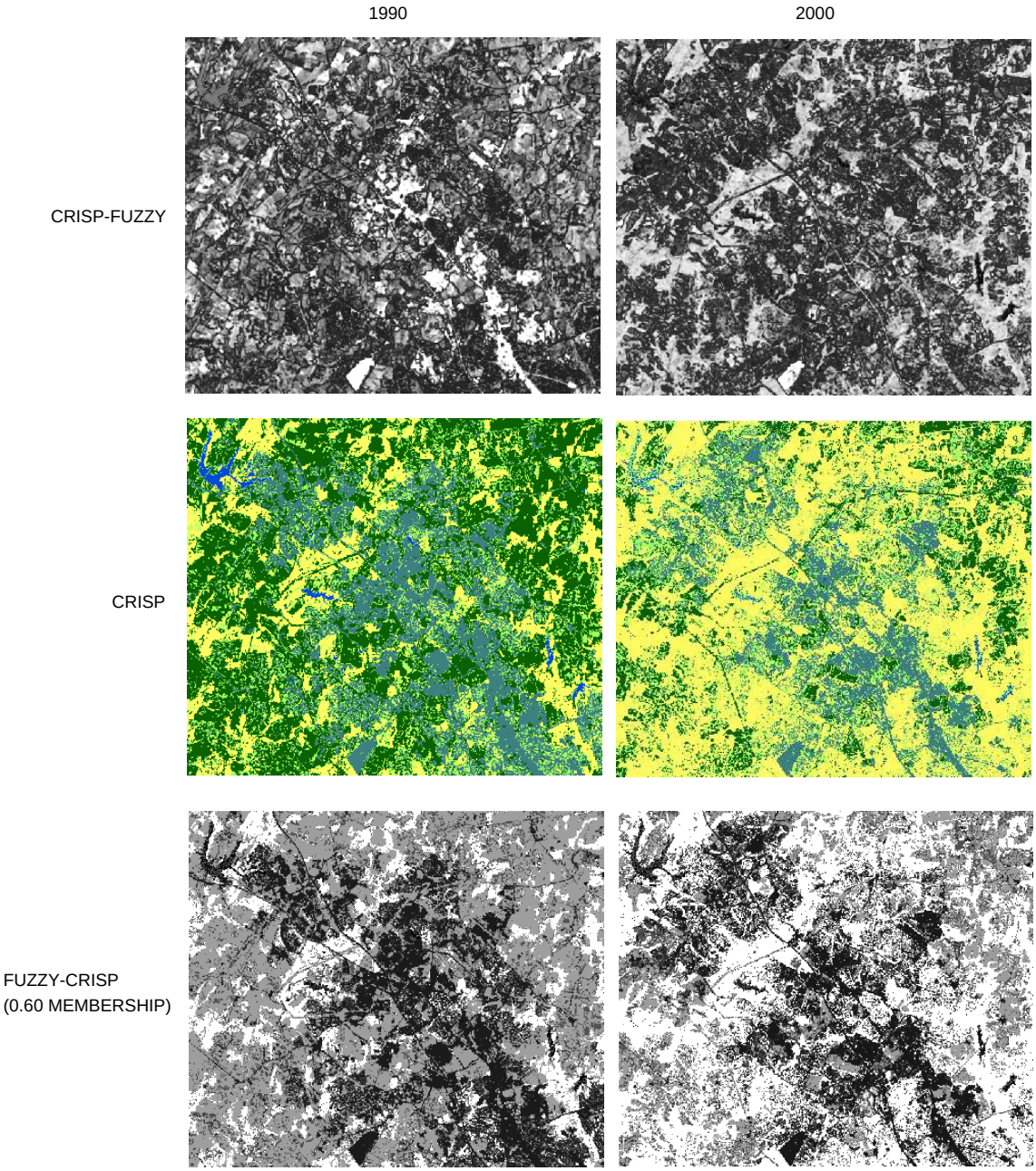

Figure 5: Image regions derived in the fuzzification stage for the 1990 and 2000 dates. From top to botton: crisp-fuzzy image regions, crisp image regions, and fuzzy-crisp image regions with threshold at 0.60 membership.

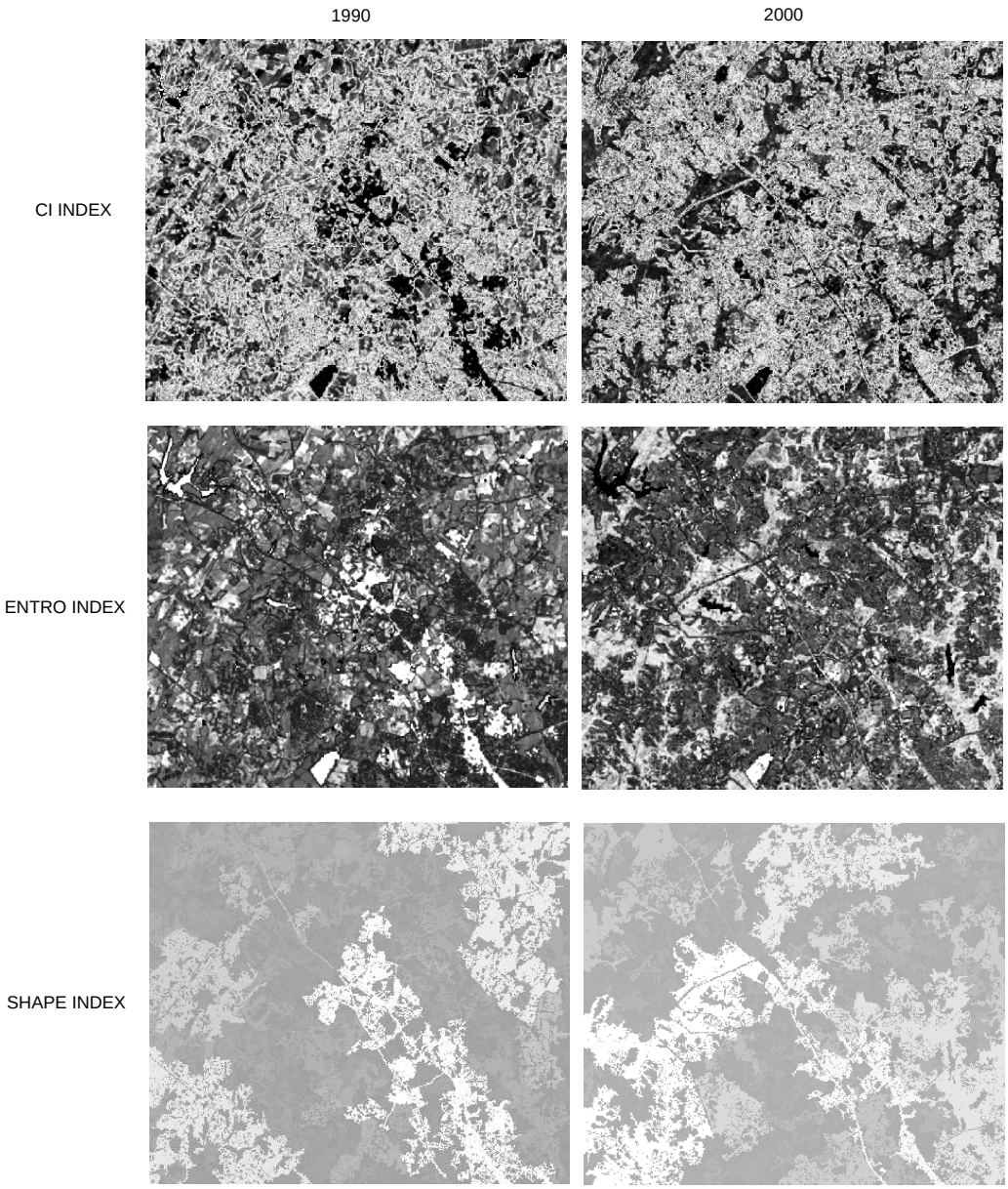

Figure 6: Contextual and spatial indices obtained from fuzzy image regions for the 1990 and 2000 dates: (a) confusion index, (b) entropy, and (c) shape index.

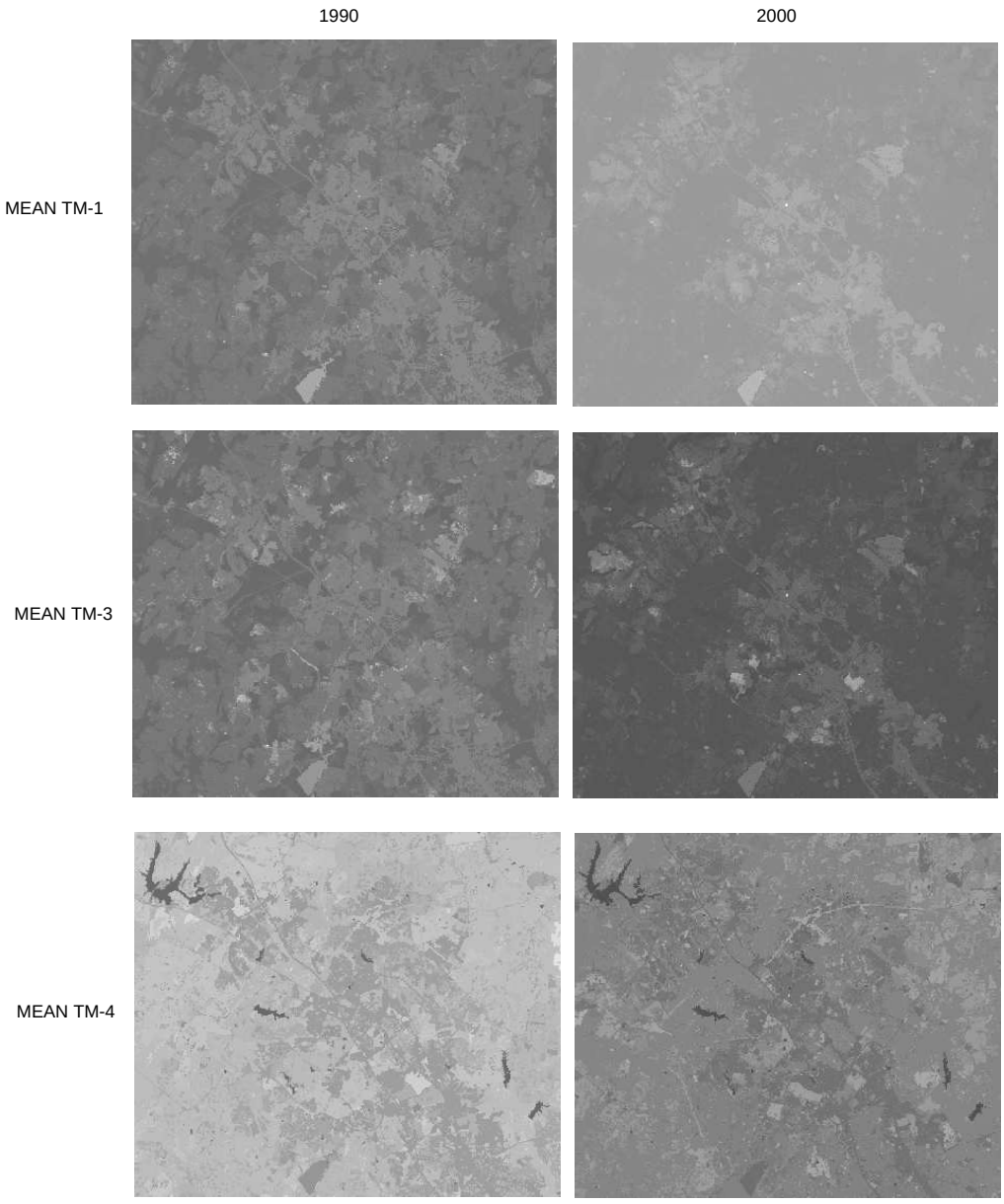

Figure 7: Spectral indices obtained from crisp image regions for the 1990 and 2000 dates: (a) mean of TM-1, (b) mean of TM-3 , and (c) mean of TM-4.

7. confusion index,
8. entropy index,
9. fuzzy crisp region at 60% threshold,
10. mean of band TM-4 within crisp image regions,
11. mean of band TM-3 within crisp image regions,
12. mean of band TM-1 within crisp image regions, and
13. shape index of crisp image regions.

A random forest (RF) technique was applied to create the impervious regression model from training samples, this time using training samples extracted from the ISA maps. A RF is a regressor that builds not one but hundreds of decision trees and combines its decisions using simple voting or advanced techniques based on consensus theory (Hastie et al., 2009). The premise is that combining many trees is often more accurate than relying on only one tree. A random forest is a collection of classification and regressionn trees (CART) following specific rules for: (i) tree growing, (ii) tree combination, (iii) self-testing, and (iv) post-processing. Each tree is grown at least partially at random: randomness is injected by growing each tree on a different random subsample of the training data. This technique, useful to create new training sets, is referred to as the bagging technique (or bootstrap aggregating). Each tree is grown on about 63% of the original training data (due to the bootstrap sampling process). Thus, the 37% of the training data is available to test any single tree. This left out data is the 'out of bag' (OOB) which allows calibration of the performance of each tree. RF have been explored for per-pixel land cover classification and experimental results suggest it is computationally more eficient and more accurate than other methods such as artificial neural networks (ANN) (Pal and Mather, 2003, Gislason et al., 2006).

The RF technique was selected due to its good performance for regression tasks in remote sensing (Walton, 2008). For creating the regression model, the RF settings were setup using default parameters as follows:

- number of trees = 500,
- number of variables to try at every split = 3.

As a final step, an evaluation of the accuracy of impervious surface mapping was conducted using the ground reference images. For such a purpose the original ISA 1990 and 2000 maps (and the urban development map), produced by WHRC at 30 m spatial resolution, were subset and resampled to 28.5 meters to match the window and pixel size of the Landsat-TM images of 28.5 m. While this resampling degrades the quality of ground reference data, it was considered a more preferable choice than coarsening the pixel size of the Landsat images.

Direct comparison between the predicted and the ground reference ISA was conducted using the Pearson's correlation coefficient (Hall, 1979). Area estimation of impervious surfaces in a given image was calculated by taking the sum of all pixel membership values for the image under consideration (Fisher et al., 2006).

Once the impervious surface areas were estimated, the subsequent task to be conducted was change analysis. *Loss* and *Gain* estimation was conducted based on the predicted impervious surfaces, using a change matrix (as suggested by (Fisher et al., 2006) for per-pixel fuzzy change analysis) to accommodate zones of *No Change* and *Change*. The diagonal cells of the change matrix indicating *no change* has occurred in a cover class C_j between time $t1$ and time $t2$ were obtained using the equation (Fisher et al., 2006):

$$\mu(C_{j[nochange]}) = min(\mu(C_{j[t1]}), \mu(C_{j[t2]})) \quad (6)$$

where min indicates the minimum operator (intersection) between fuzzy sets, i.e. the minimum value of the membership values $\mu(C_{j[ti]})$ to class C_j for a given time $t1$ or $t2$.

Gain, the total area of class j which is gained, is given by the areas which are not members of class (C_j) at time $t1$, denoted as $\mu(\neg C_{j[t1]})$ and are members of class (C_j) at time $t2$, denoted as $\mu(C_{j[t2]})$. Gain was calculated using the equation (Fisher et al., 2006):

$$\mu(C_{j[gain]}) = max(0, \mu(\neg C_{j[t1]}) + \mu(C_{j[t2]}) - 1) \quad (7)$$

where max indicates the maximum operator (union) between fuzzy sets, i.e. the maximum value of each membership value to a given class $\mu(C_j)$.

Loss, the total area of class j which is lost, is given by the areas which are members of class (C_j) at time $t1$, denoted as $\mu(C_{j[t1]})$, and are not members of class (C_j) at time $t2$, denoted as $\mu(\neg C_{j[t2]})$. Loss was calculated using the equation (Fisher et al., 2006):

$$\mu(C_{j[loss]}) = max(0, \mu(C_{j[t1]}) + \mu(\neg C_{j[t2]}) - 1) \quad (8)$$

The off-diagonal cells representing change in the change matrix were calculated as the intersection of the gain in class C_j and the loss in class C_k over the interval $t1$ to $t2$ using the equation (Fisher et al., 2006):

$$\mu(C_{j[change]}) = min(\mu(C_{j[gain]}), \mu(C_{k[loss]})) \quad (9)$$

All the processes for quantitative classification were implemented by using R (Team, 2008) and $SAGAGIS$ (). Besides the R base package, the following libraries were used to develop the method: $rgdal$, sp, $spatstats$, $maptools$, $RSAGA$, gam and $randomForest$.

4 RESULTS

Figures 8 (a) and (b) show the impervious surface areas (ISA) maps in 1990 and 2000 as predicted using the FIRME approach with a random sample of 2000 pixels which represent 0.54 % of the study area.

The Pearson's correlation coefficient (Hall, 1979) between the predicted ISA images and the ground reference images, shown in Figures 8 (c) and (d), are 0.76 and 0.81 respectively. It is a good approximation to the real impervious surface, and minor misprediction problems are detected only after a careful visual assessment. As Table 1 shows, GAM-RF based fuzzy segmentation overestimates impervious surface by 7.3% and 6.1% respectively. Table 1 also shows that the correlation coefficient between

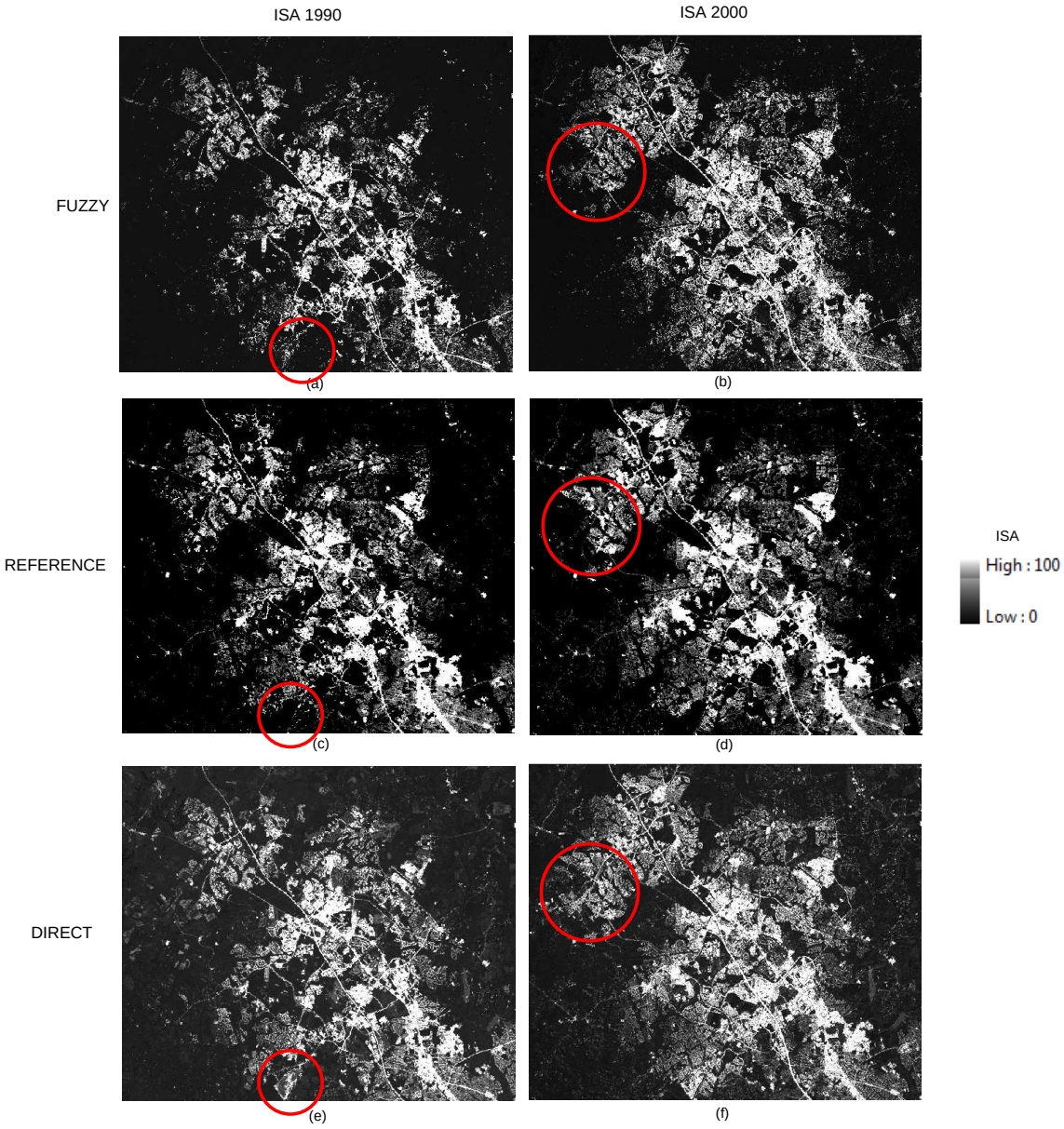

Figure 8: Impervious surface area (ISA) maps for the study area using: (a) FIRME method 1990, (b) FIRME method 2000, (c) Reference data 1990, (d) Reference data 2000, (e) DIRECT method 1990, and (f) DIRECT method 2000.

the ISA change predicted by the FIRME method and the actual change is 0.49. The fuzzy segmentation method overestimates ISA change by 10.13%.

As this study aimed at analyzing the contribution of fuzzy image region to increasing the accuracy of the ISA estimation, a direct regression was tested. A direct regression uses the SVM technique for estimation of impervious surface area values directly from the normalized spectral bands. In this option, the fuzzy segmentation and feature analysis stages are omitted, and the estimation relies only on a reliable quantitative training sample, and on the predictive power of SVM. Figures 8 (e) and (f) show the ISA maps obtained using direct regression (DIRECT). In Figure 8 red coloured circles at each ISA map highlight zones of major misprediction where bare soil zones are taken as impervious surfaces. Table 1 also presents the results obtained using the direct regression option. It is apparent that the fuzzy segmentation method outperforms the DIRECT method. Note that, for individual dates, the area error using the FIRME method is about 3 times lower than the area error using the DIRECT method. With regard to change in ISA values, the FIRME METHOD is about three times more accurate than the DIRECT method.

Figure 9 (a) shows the predicted change on impervious surface area (ISA) values from 1990 to 2000 using the FIRME method with training sample size of 2000 pixels. Figure 9 (b) shows the urban development reference data (Jantz et al., 2005). Figure 9 shows that, using the proposed method, a general overestimation occurs over the whole study area. As Table 1 shows, the FIRME method overestimates urban development surface by 13%.

Table 2 shows, on the other hand, the relative importance of each predictor variable to create the Random Forest (RF) regression model for estimating impervious surface at the final regression stage. Although RF needs manual parameterisation, its results do not change too much depending on the values assigned to the number of trees or on the number of variables tried at every split. The importance of predictor variables in RF is reported using the *IncMSE* value. This means that, for each tree, the prediction accuracy is calculated *with* and *without* each predictor variable using the *mean squared error*. Then, the differences in accuracy are averaged over all trees and normalized by the standard error. If the standard error is equal to 0 for a given variable, the division is not done but the reported value is 0. In short, a low value of *IncMSE* means that the corresponding predictor has low importance. According to Table 2, it is apparent that the water fuzzy region, the crisp image regions and the fuzzy-crisp image regions at 0.60 threshold are not very important in any of the two models. Conversely, the remaining fuzzy image regions seems to be important predictors. In particular, fuzzy image region urban, crisp-fuzzy image regions, and shape index of crisp image regions are very important in the two models. Interestingly, the fuzzy region bare soil is important for the 1990 model but is not for the 2000 model. This could be explained by the existence, in 1990, of a bare soil zone which is spectrally similar to impervious surface. This zone is shown inside the red coloured circle in Figure 8 (a), (c), and (e). Apart from such difference, it seems that the importance values show low change between regression models. This fact suggests that the *IncMSE* values provide information useful to understand, to some degree, what is happening inside a given RF regression model.

5 DISCUSSION

The degree of agreement between the impervious surface area (ISA) values predicted and the actual ISA data (i.e. the ground reference data) covering the study area may be considered as good for a range of environmental studies. The proposed method may be used as a rapid means for quantitative classification and change estimation. However, additional refining of results using ground data may be necessary for resolving eventual inaccuracies.

For comparison purposes, an additional test was conducted in this experiment to estimate how sensitive the fuzzy segmentation approach is to the algorithm used for the fuzzification, and respectively, defuzzification stage. In the test, the same procedure explained earlier was applied but using the support vector machine (SVM) technique (i.e. SVM was applied for both fuzzification and defuzzification) instead of the GAM-RF combination.

SVM is a widely used machine learning method for per-pixel image classification (Foody and Mathur, 2004, Huang et al., 2002, Zhu and Blumberg, 2002). SVM transforms the input data set into a higher-dimensional space using special functions called kernels. SVM uses the *structural risk minimisation*(SRM) principle to find a separating hyperplane which minimizes the margin between two classes (Duda et al., 2001).

The SVM approach for solving the two classes problem can be extended to multiclassification tasks (Duda et al., 2001). Moreover, the SVM technique can be also applied to regression problems. In SVM regression, the goal is to find a function $f(x)$ that has at most a given deviation, referred to as ϵ, from the actually obtained targets y_i for all the training data, and at the same time is as flat as possible. In other words, errors, i.e. the differences between y_i and $f(x)$, are not important as long as they are less than ϵ, but will not be accepted if they are larger than this (Smola and Scholkopf, 2003).

Kernel functions commonly used in SVM are: (i) polynomial, (ii) radial basis function, and (iii) sigmoid. SVM requires only small training samples to fit the classification or regression model. Also, while SVM parameterisation is considered to be a complex issue, it can be solved using automatic procedures (Smola and Scholkopf, 2003).

Table 3 shows the performance of the method when applying SVM, using a radial basis function and an automated parameterisation strategy (Lizarazo, 2008), in order to estimate urbanization changes. It can be noted that area error values and correlation indices are similar for both the GAM-RF and the SVM-SVM combinations. Figure 10 shows the ISA images predicted using the GAM-RF and the SVM-SVM techniques. It is apparent that these SVM estimates are qualitatively superior to those obtained using the GAM-RF combination, and visually more appealing, because SVM is able to better resolve the spectral confusion between bare soil areas and impervious surface areas. As noted in an earlier paper (Lizarazo, 2008), a main drawback of the SVM technique is that it provides little information about the importance of individual predictors.

The FIRME method can be extended easily to accommodate the estimation of other land cover surface areas as needed in a particular study. Although the implementation reported in this paper used a GAM & RF combination (and also a SVM & SVM combination), the method can be modified for any machine learning technique. The main advantages of the method are its simplicity and transferability. The only particular requirement of the fuzzy image regions method (FIRME) is the collection of accurate samples to train the two regression tasks involved in the method.

Results from this experiment show that the FIRME approach is a suitable alternative for quantitative land cover estimation. Compared with much more established techniques (Clapham, 2005,

Table 1: Comparison between the fuzzy image regions method (FIRME) and the direct regression method (DIRECT) for obtaining impervious surface areas. Training sample is 2000 pixels. Area error was calculated as the ratio between predicted area and actual area.

Test	correlation coefficient	95% confidence interval	Area error (%)
ISA 1990			
FIRME	0.71	[0.695, 0.716]	+ 7.3
DIRECT	0.69	[0.688, 0.703]	+ 21.2
ISA 2000			
FIRME	0.75	[0.738, 0.765]	+ 6.1
DIRECT	0.73	[0.715, 0.748]	+ 22.9
CHANGE			
FUZZY	0.494	[0.481 , 0.503]	+ 10.1
DIRECT	0.393	[0.381 , 0.405]	+ 33.8

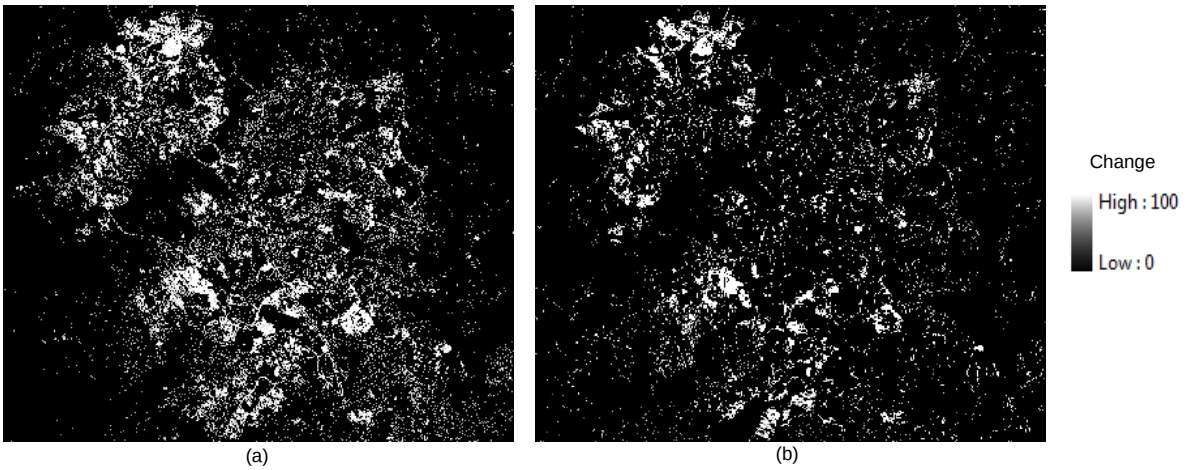

(a) (b)

Figure 9: Change on impervious surface area (ISA) values from 1990 to 2000: (a) as predicted using the FIRME method (GAM-RF techniques), (b) as represented in the ground reference data.

Table 2: Importance of predictor variables (measured as IncMSE value) using the fuzzy segmentation approach and applying the combination GAM-RF. Sample size comprises of 2000 pixels. *imgreg* stands for image region.

Predictor	ISA 1990 Model	ISA 2000 Model
Fuzzy imgreg water	8.75	5.86
Fuzzy imgreg urban	34.13	27.26
Fuzzy imgreg grass	24.77	15.07
Fuzzy imgreg trees	23.21	31.11
Fuzzy imgreg bare soil	24.86	14.53
crisp imgreg	14.11	13.20
crisp-fuzzy imgreg	31.72	34.71
confusion index	29.74	33.14
entropy index	38.67	40.24
fuzzy-crisp imgreg at 0.60	15.47	11.67
mean of TM-4 at crisp imgreg	28.23	20.56
mean of TM-3 at crisp imgreg	21.17	20.43
mean of TM-1 at crisp imgreg	24.31	17.64
shape index of crisp imgreg	27.91	30.73

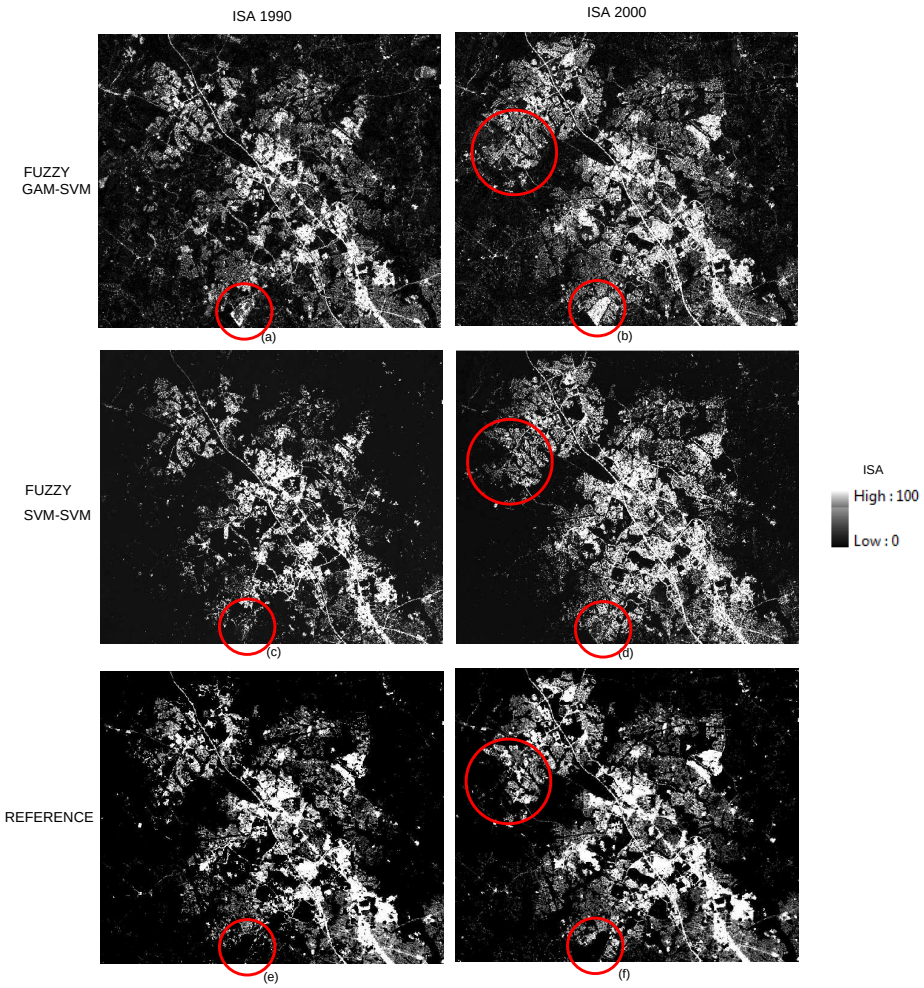

Figure 10: ISA prediction using the fuzzy segmentation approach: (a) GAM-RF, (b) SVM-SVM, (c) Reference data.

Table 3: Comparison between two machine learning techniques for estimation of impervious surface areas using the fuzzy image regions method (FIRME). Training sample is 2000 pixels. Area error was calculated as the increase (+) or decrease (-), measured in percentage, between predicted area and reference area.

Test	Correlation index	95% confidence interval	Area error (%)
ISA 1990			
GAM-RF	0.76	[0.763, 0.766]	+7.3
SVM-SVM	0.75	[0.748, 0.756]	+7.6
ISA 2000			
GAM-RF	0.80	[0.798, 0.804]	+6.1
SVM-SVM	0.79	[0.784, 0.795]	+7.5
CHANGE			
GAM-RF	0.494	[0.481 , 0.503]	+10.1
SVM-SVM	0.509	[0.503 , 0.514]	+11.2

Jantz et al., 2005), it is much more simple to apply, and it is less dependent on manual procedures such as visual interpretation of of land cover classes, visual-screening, or land cover masking. Unlike those approaches, the fuzzy segmentation approach requires a relatively low number of training samples. Accuracy of impervious surface area values obtained using FIRME are acceptable for most practical purposes. However, as this accuracy was obtained using ground reference data obtained by (Jantz et al., 2005), and, an independent validation sample was not available, it was not possible to draw conclusions about the relative performance between the fuzzy segmentation approach and that method in terms of thematic accuracy.

6 CONCLUSIONS

This paper devised and tested a method for quantitative land cover mapping using fuzzy image regions. It was shown how important are fuzzy image regions as predictors of quantitative values of impervious surfaces. It was demonstrated that fuzzy image regions hold a potential richness of information which can help to reduce spectral confusion between land cover classes.

Experimental results show that GAM-RF based fuzzy image regions provide more accurate estimation of impervious surface areas than a direct RF regression method. The GAM and RF techniques provide similar accuracies than the SVM regression and are computationally affordable for processing large data sets. While the FIRME method is highly dependent on accurate training samples, it is simple to use and may be used to obtain reliable estimates of ISA values and urbanization changes.

This study suggests that fuzzy segmentation is a useful framework for conducting compositional land cover classification. As quantitative classification is not a very common task in GEOBIA, the FIRME method shows a great potential for moving geographic object-based image analysis beyong its current boundaries. It can be stated therefore that fuzzy image regions may contribute to bridge the gap between the traditional quantitative and qualitative perspectives of remote sensing image analysis which are often seen as two different and independent worlds .

ACKNOWLEDGEMENTS

The author would like to thank Dr Scott Goetz (Woods Hole Research Center, USA) who provided him with the ISA 1990, ISA 2000 and urban datasets used as ground reference. The author also thanks to the Centro de Investigacion y Desarrollo Cientifico (Universidad Distrital, Colombia) who supported his participation in GEOBIA 2010.

REFERENCES

Arnold, C. and Gibbons, J., 1996. Impervious surface coverage: The emergence of a key environmental indicator. C. Arnold and J. Gibbons 62, pp. 243–258.

Bragato, G., 2004. Fuzzy continuous classification and spatial interpolation in conventional soil survey for soil mapping of the lower piave plain. Geoderma 118, pp. 1–16.

Brown, D. G., Goovaerts, P., Burnicki, A. and Li, M.-Y., 2002. Stochastic simulation of land-cover change using geostatistics and generalized additive models. Photogrammetric Engineering & Remote Sensing 68(10), pp. 10511061.

Burrough, P., van Gaans, P. and Hoostmans, R., 1997. Continuous classification in soil survey: spatial correlation, confusion and boundaries. Geoderma.

Clapham, W. B., 2005. Quantitative classification as a tool to show change in an urbanizing watershed. International Journal of Remote Sensing 26(22), pp. 4923–4939.

Duda, R., Hart, P. and Stork, D., 2001. Pattern Classification. Wiley Interscience.

Fisher, P. and Arnot, C., 2007. Geographic Uncertainty in Environmental Security. Springer, chapter Mapping Type 2 Change in Fuzzy Land Cover, pp. 167–186.

Fisher, P., Arnot, C., Wadsworth, R. and Wellens, J., 2006. Detecting change in vague interpretations of landscapes. Ecological Informatics 1, pp. 163–178.

Foody, G. M. and Mathur, A., 2004. A relative evaluation of multiclass image classification by support vector machines. IEEE Transactions on Geoscience and Remote Sensing 42, pp. 1336–1343.

Gislason, P. O., Benediktsson, J. A. and Sveinsson, J. R., 2006. Random Forests for land cover classification. Pattern Recognition Letters 27(4), pp. 294–300.

Goetz, S. J. and Jantz, P., 2006. Satellite Maps Show Chesapeake Bay Urban Development. EOS Transactions American Geophysical Union 87(15), pp. 149–156.

Gonzalez, R., 2008. Digital Image Processing. Third edition edn, Prentice Hall.

Hall, E. H., 1979. Computer Image Processing and Recognition. Academic Press.

Hastie, T., Tibshirani, R. and Friedman, J., 2009. The Elements of Statistical Learning: Data Mining, Inference and Prediction. Springer.

Hay, G. J. and Blaschke, T., 2010. Special issue: Geographic object-base image analysis. Photogrammetric Engineering & Remote Sensing 76(2), pp. 121–122.

Huang, C., Davis, L. and Townshend, J. R. G., 2002. An assessment of support vector machines for land cover classification. International Journal of Remote Sensing 23, pp. 725–749.

Jantz, P., Goetz, S. and Jantz, C., 2005. Urbanization and the loss of resource lands in the chesapeake bay watershed. Environmental Management 36(6), pp. 808–825.

Jensen, J., 2005. Introductory Image Processing: a Remote Sensing perspective. Prentice Hall.

Johansen, K., Arroyo, L. A., Phinn, S. and Witte, C., 2010. Comparison of geo-object based and pixel-based change detection of riparian environments using high spatial resolution multispectral imagery. Photogrammetric Engineering & Remote Sensing 76(2), pp. 123–136.

Kim, M., Madden, M. and Xu, B., 2010. Geobia vegetation mapping in great smoky mountains national park with spectral and non-spectral ancillary information. Photogrammetric Engineering & Remote Sensing 76(2), pp. 137–149.

Lizarazo, I., 2008. SVM-based segmentation and classification of remotely sensed data. International Journal of Remote Sensing 29(24), pp. 7277–7283.

Lizarazo, I., 2010. Fuzzy image regions for estimation of impervious surface areas. Remote Sensing Letters 1(1), pp. 19–27.

Lizarazo, I. and Barros, J., 2010. Fuzzy image segmentation for urban land cover classification. Photogrammetric Engineering & Remote Sensing 76(2)(2), pp. 151–162.

Opsomer, J. D., Jay, B. F., Moisen, G. G. and Kauermann, G., 2007. Model-assisted estimation of forest resources with generalized additive models. Journal of the American Statistical Association 100, pp. 400–416.

Pal, M. and Mather, P. M., 2003. An assessment of the effectiveness of decision tree methods for land cover classification. Remote Sensing of the Environment 86, pp. 554–565.

Ross, T., 2004. Fuzzy Logic with Engineering Applications. Wiley.

Smola, A. J. and Scholkopf, B., 2003. A tutorial on support vector regression. Technical report, NeuroCOLT2 Technical Report Series.

Team, R., 2008. An introduction to R. Available at http://www.r-project.org/.

Walton, J. T., 2008. Subpixel urban land cover estimation: Comparing cubist, random forests, and support vector regression. Photogrammetric Engineering & Remote Sensing 74(10), pp. 1213–1222.

Weng, Q., 2007. Remote sensing of impervious surfaces: An overview. In: T. . F. Group (ed.), Remote Sensing of Impervious Surfaces, Taylor and Francis.

Wood, S., 2006. Generalized Additive Models: an introduction with R. Chapman and Hall.

Zhu, G. and Blumberg, D. G., 2002. Classification using ASTER data and SVM algorithms: the case study of Beer Sheva, Israel. Remote Sensing of the Environment 80, pp. 233–240.